Supplementary Data.

Laraba et al.

Title: **Inhibition of YAP/TAZ-driven TEAD activity prevents growth of NF2-null schwannoma and meningioma.**

This file includes Supplementary Methods together with Supplementary Figures 1-11 plus their corresponding legends and references.

Supplementary Methods.

RNA extraction and gene expression analysis

Mouse sciatic nerve and DRGs were dissected into RNA*later*™(ThermoFisher; AM7020), RNA was extracted using Qiazol (Qiagen; 79306) and the miRNeasy Micro Kit (Qiagen; 217084) according to manufacturer's instructions. cDNA was prepared using the reverse transcription system (Promega; A3500), according to manufacturer's instructions to generate cDNA. Taqman® qPCR was performed as described previously[1] with the following probes and targets: *actb* (Mm02619580_g1); *aldh1a1* (Mm00657317_m1); *birc5* (Mm00599749_m1); *ctgf* (Mm01192933_g1); *cyr61* (Mm00487498_m1); *igfbp2* (Mm00492632_m1) and *mrpl10* (Mm00452706_m1). Gene expression was quantified in sciatic nerve against the housekeeping gene *mrpl10*[2] and for DRG against the housekeeping gene *actb* (beta-actin). Gene expression was quantified in triplicate using the $2^{-(\Delta\Delta Ct)}$ method, made relative to the CRE- vehicle control. The Rosa TdTomato strain and its use has been previously described[3].

Suppl. Figure 1

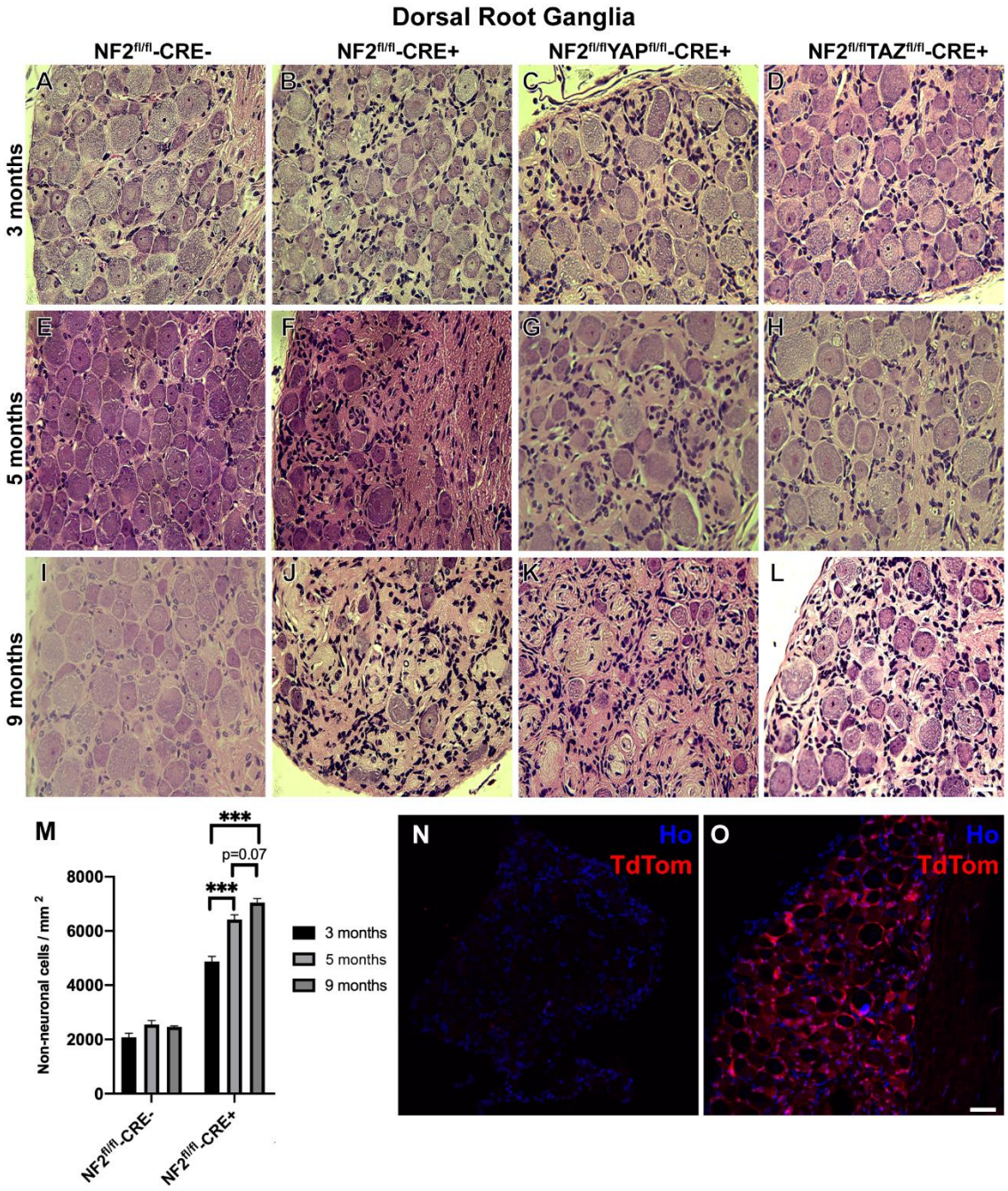

Supplemental Figure 1: Increasing hyperplasia of Schwann cells within dorsal root ganglia (DRGs) of NF2-null mice with age. A-L. Haematoxylin & Eosin stained paraffin sections of Control ($NF2^{fl/fl}$-CRE-) (A, E, I), NF2 single null ($NF2^{fl/fl}$-CRE+) (B, F, J), NF2/YAP double null ($NF2^{fl/fl}YAP^{fl/fl}$-CRE+) (C, G, K) and NF2/TAZ double null ($NF2^{fl/fl}TAZ^{fl/fl}$-CRE+) (D, H, L) DRG tissue at 3, 5 and 9 months. Note increasing hyperplasia in NF2 single null tissue between 3 (B), 5 (F) and 9 (J) months. M. Quantification of numbers of non-neuronal cell nuclei per area in control and NF2 single null DRG tissue at 3, 5 and 9 months. N, O. Representative images showing fluorescence of TdTomato (TdTom, red; Hoechst (Ho) counterstain in blue) in sections of DRG tissue from PostnCRE- /TdTomato (N) and PostnCRE+/TdTomato (O) adult mice. For data presented, n=3 for all timepoints and genotypes. Data presented are means ±SEM. Statistical analysis shown in M is a two-way ANOVA (repeated measures), using Tukey's multiple comparisons test. *** $P<0.001$. Scale bar 25 μm.

Suppl. Figure 2

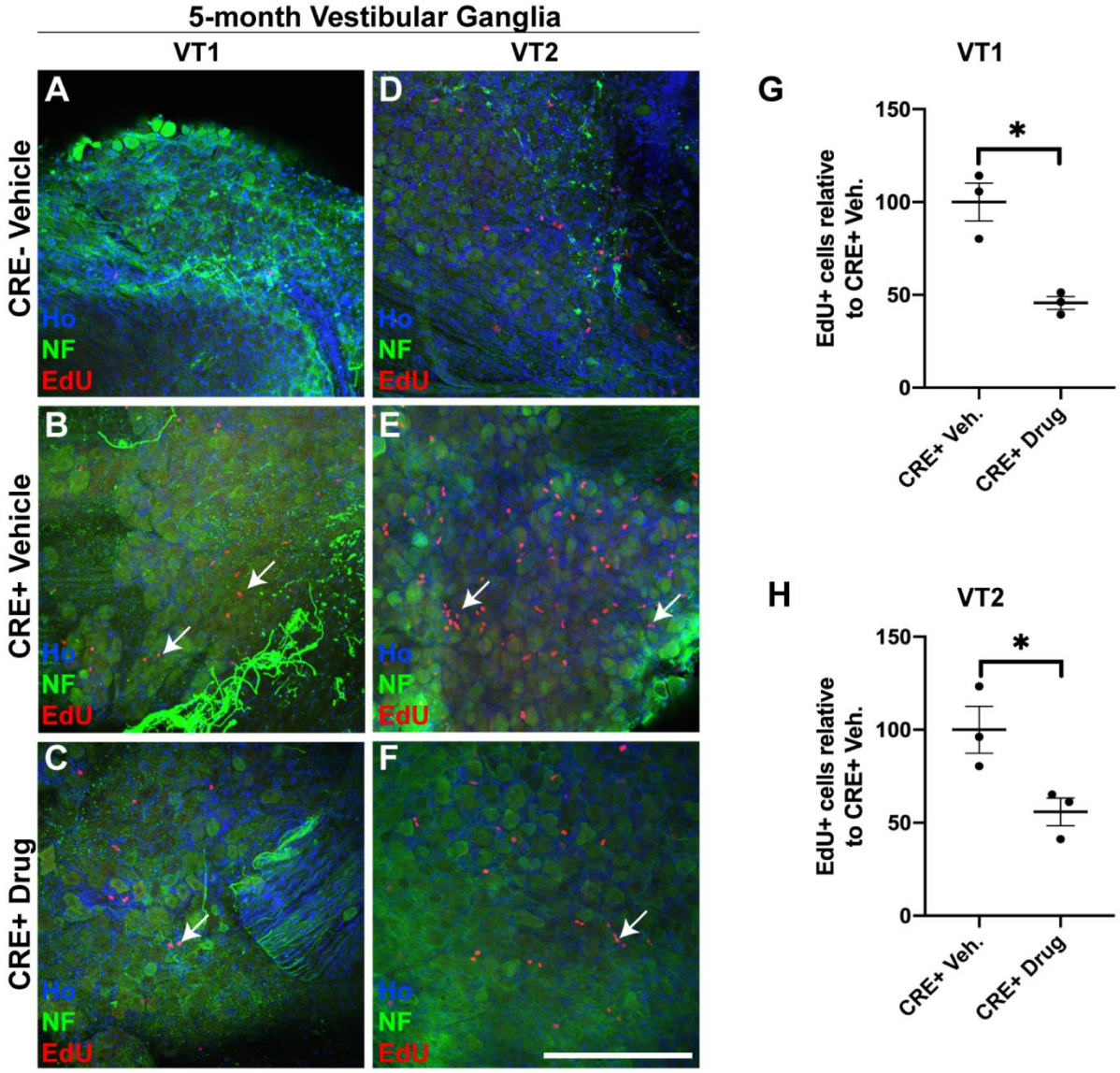

Supplementary Figure 2: Treatment of mice with VT1 or VT2 TEAD auto-palmitoylation inhibitors significantly inhibits growth of vestibular ganglia (VG) schwannoma tumours *in vivo*. Data from 5 month old $NF2^{fl/fl}$ PostnCRE- (CRE-) and $NF2^{fl/fl}$ PostnCRE+ (CRE+) animals treated with 10mg/kg/day VT1 or 30mg/kg/day VT2 by oral gavage for 21 consecutive days. A-H. Both VT1 and VT2 significantly block tumour cell growth as measured by EdU incorporation in VG tissue. A-F. Images of VG tissue from CRE- and CRE+ animals treated with either vehicle (A, B, D and E), VT1 (C) or VT2 (F). Note that for CRE+ animals, numbers of EdU positive cells (indicated by arrows) are reduced upon treatment with either VT1 (C) or VT2 (F). G, H. Quantification of numbers of EdU positive cells per area of VG tissue from animals treated with vehicle (Veh.) or VT1 (Drug; G) or VT2 (Drug; H) compounds. Note significant decreases in proliferation in CRE+ animals treated with either VT1 or VT2. For data in A-H, n=3 mice for each genotype and drug treatment. Data presented in graphs are means ±SEM using one way ANOVA with Bonferroni's multiple comparison tests. * $P<0.05$. Scale bar: 200 μm.

Suppl. Figure 3

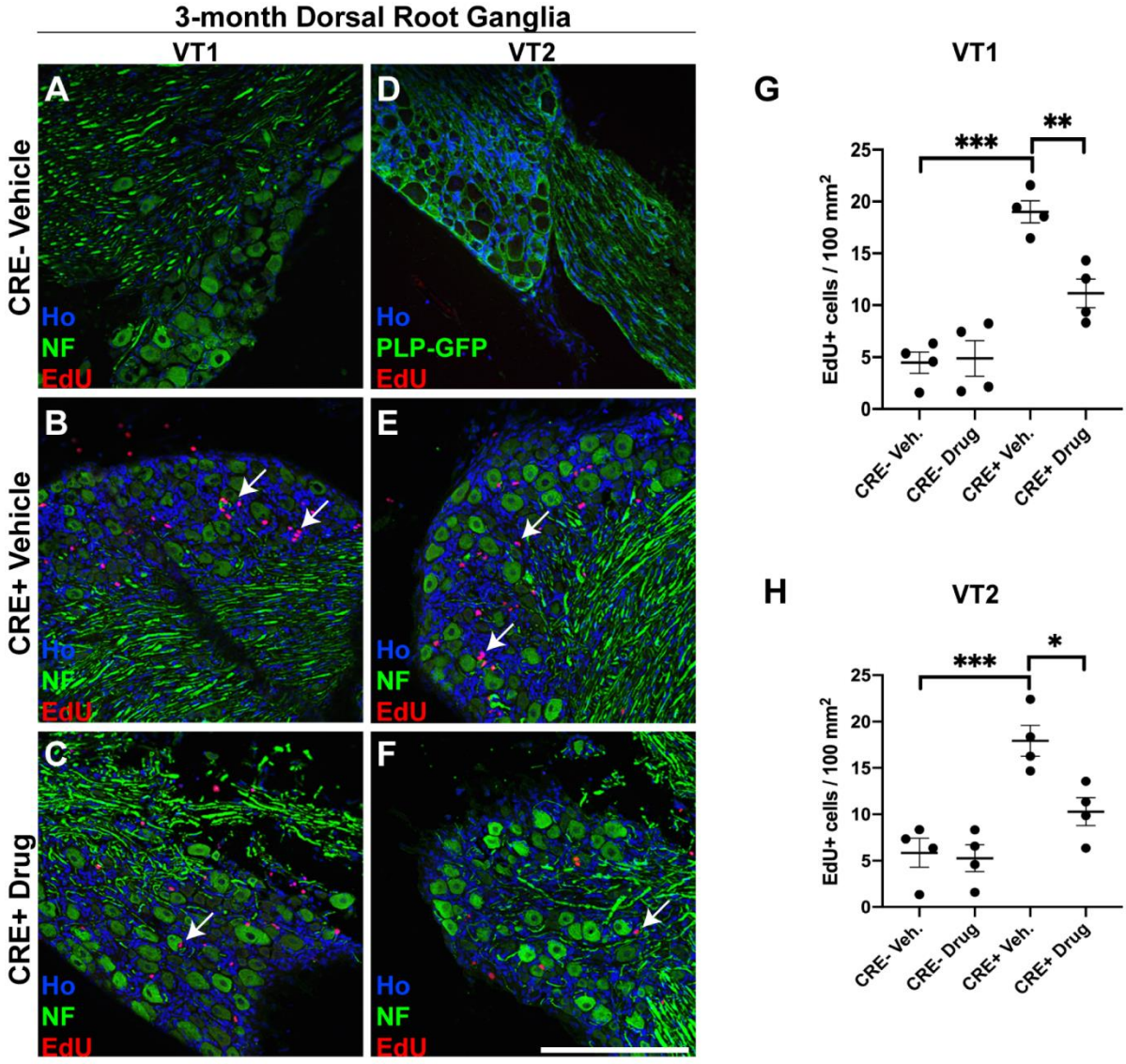

Supplementary Figure 3: Treatment of mice with VT1 or VT2 TEAD auto-palmitoylation inhibitors significantly inhibits growth of dorsal root ganglion (DRG) schwannoma tumours *in vivo*. Data from 3 month old $NF2^{fl/fl}$ PostnCRE- (CRE-) and $NF2^{fl/fl}$ PostnCRE+ (CRE+) animals treated with vehicle (Veh), 10mg/kg/day VT1 or 30mg/kg/day VT2 by oral gavage for 21 consecutive days. A-H. Both VT1 and VT2 significantly block tumour cell growth as measured by EdU incorporation in DRG tissue. A-F. Images of DRGs from CRE- and CRE+ animals treated with either vehicle (A, B, D and E), VT1 (C) or VT2 (F). Note that for CRE+ animals, numbers of EdU positive cells (indicated by arrows) are reduced upon treatment with either VT1 (C) or VT2 (F). G, H. Quantification of numbers of EdU positive cells per area of ganglion tissue from animals treated with vehicle (Veh.) or VT1 (Drug; G) or VT2 (Drug; H) compounds. Note significant decreases in proliferation in CRE+ animals treated with either VT1 or VT2. For data in A-H, n=4 mice for each genotype and drug treatment. Data presented in graphs are means ±SEM. Analysis was done using one way ANOVA with Bonferroni's multiple comparison tests. * $P<0.05$; ** $P<0.01$; *** $P<0.001$. Scale bar: 200 μm.

Suppl. Figure 4

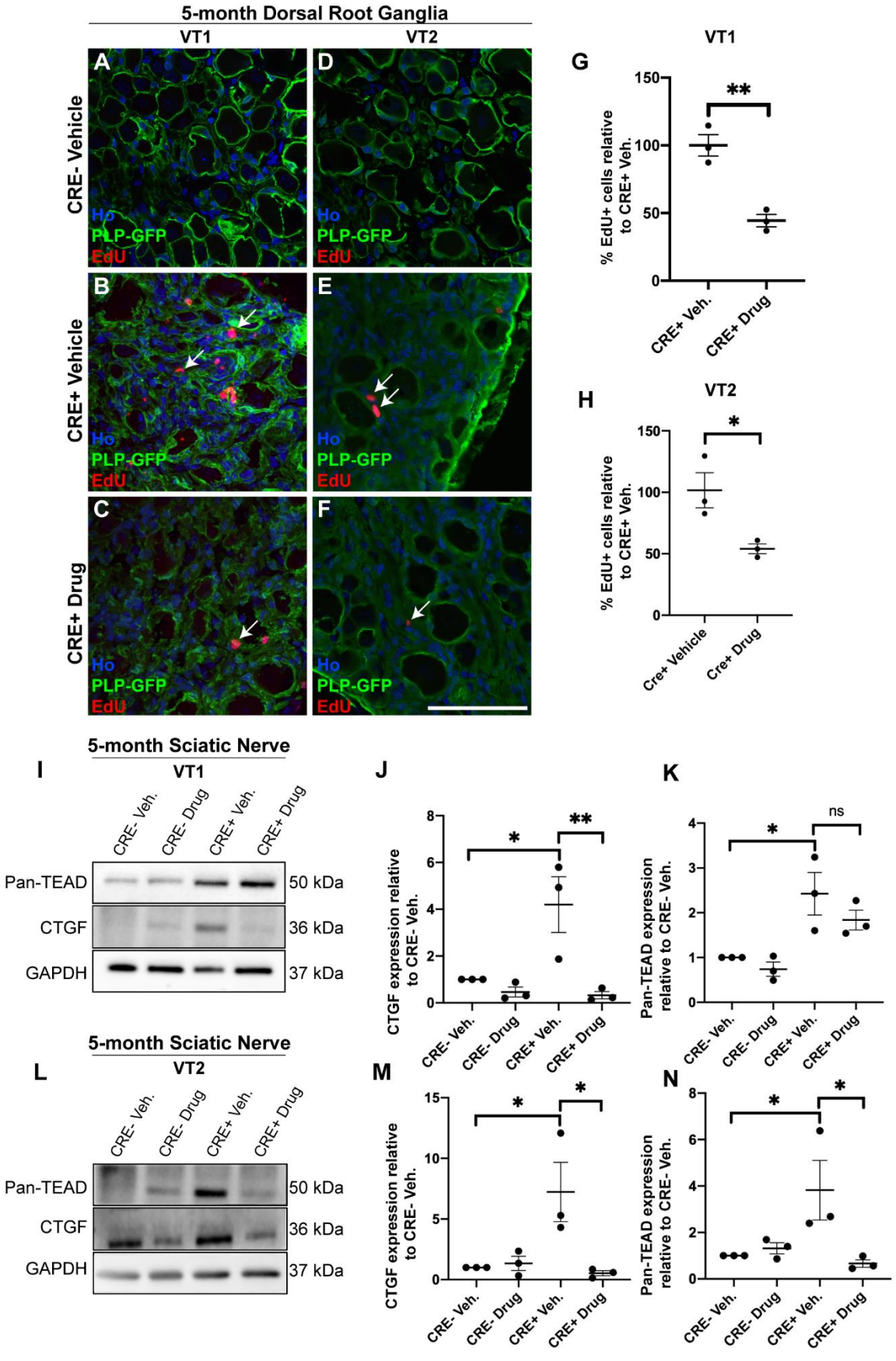

Supplementary Figure 4: Treatment of mice with VT1 or VT2 TEAD auto-palmitoylation inhibitors significantly inhibits proliferation of dorsal root ganglion (DRG) schwannoma tumours *in vivo*. Data from 5 month old $NF2^{fl/fl}$ Postn-CRE-/PLP-GFP+ (CRE-) and $NF2^{fl/fl}$ Postn-CRE+ PLP-GFP+ (CRE+) animals treated with 10mg/kg/day VT1 or 30mg/kg/day VT2 by oral gavage for 21 consecutive days. A-H. Both VT1 and VT2 significantly block tumour cell proliferation as measured by EdU incorporation in DRG tissue. A-F. Images of DRG tissue from CRE- and CRE+ animals treated with either vehicle (A, B, D and E), VT1 (C) or VT2 (F). Note no EdU positive cells are seen in CRE- animals with vehicle and that for CRE+ animals, numbers of EdU positive cells (indicated by arrows) are reduced upon treatment with either VT1 (C) or VT2 (F). G, H. Quantification of numbers of EdU positive cells per area of DRG tissue from animals treated with vehicle (Veh.) or VT1 (Drug; G) or VT2 (Drug; H) compounds. Note significant decreases in proliferation in CRE+ animals treated with either VT1 or VT2. I-N. Representative western blots and quantification to show target engagement of VT1 and VT2 in regulating CTGF and TEAD protein expression in sciatic nerve tissue of 5 month old CRE- and CRE+ mice. I, L. Western blots of sciatic nerve of 5 month old mice treated for 21d with either Vehicle (Veh.) or VT1 (Drug; I), or Vehicle or VT2 (Drug; L). J, K. Quantification of western blot in I. M, N. Quantification of western blot in L. Note significant decrease in TEAD target CTGF by both VT1 and VT2 in sciatic nerve tissue in vivo (J, M) and reduction in TEAD protein expression by VT2 (N) but not by VT1 (K). For data in A-H, n=4 mice for each genotype and drug treatment. For the remaining data in this Figure (I-N), n=3 mice for each genotype and drug treatment. Data presented in graphs are means ±SEM using one way ANOVA with Bonferroni's multiple comparison tests. * $P<0.05$; ** $P<0.01$; ns non-significant. A-F. Scale bar: 50 μm.

Suppl. Figure 5

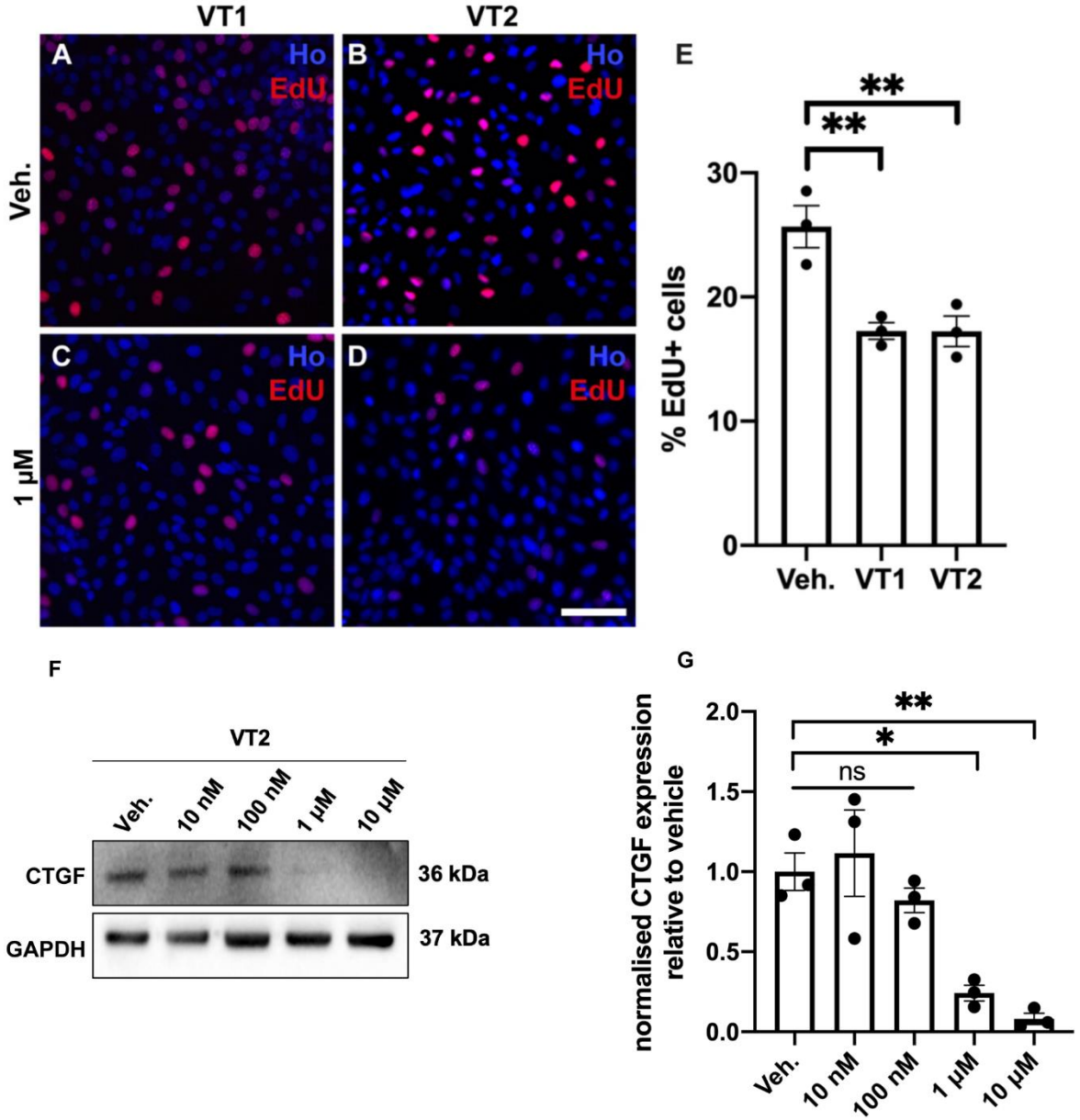

Supplementary Figure 5: TEAD auto-palmitoylation inhibitors VT1 and VT2 block proliferation of human HEI-193 NF2-null schwannoma cells. A-D. EdU labelling of HEI-193 cells treated with vehicle (A, B) or 1μM VT1 (C) or VT2 (D) compounds. Hoechst counterstain was used to reveal nuclei. E. Quantification of % EdU positive cells. F. Representative western blot of (n=3) HEI-193 cells treated for 7d with increasing concentrations of VT2 showing target engagement by downregulating the protein expression of the TEAD target gene connective tissue growth factor (CTGF). G. Quantification of CTGF levels in F, normalised to GAPDH and are relative to the vehicle control. For data in A-G, n=3. Data presented in E are means ±SEM using one way ANOVA with Bonferroni's multiple comparison tests. Data presented in G are one way ANOVA with Sidak's multiple comparison test. * $P<0.05$; ** $P<0.01$. Scale bar: 25 μm.

Suppl. Figure 6

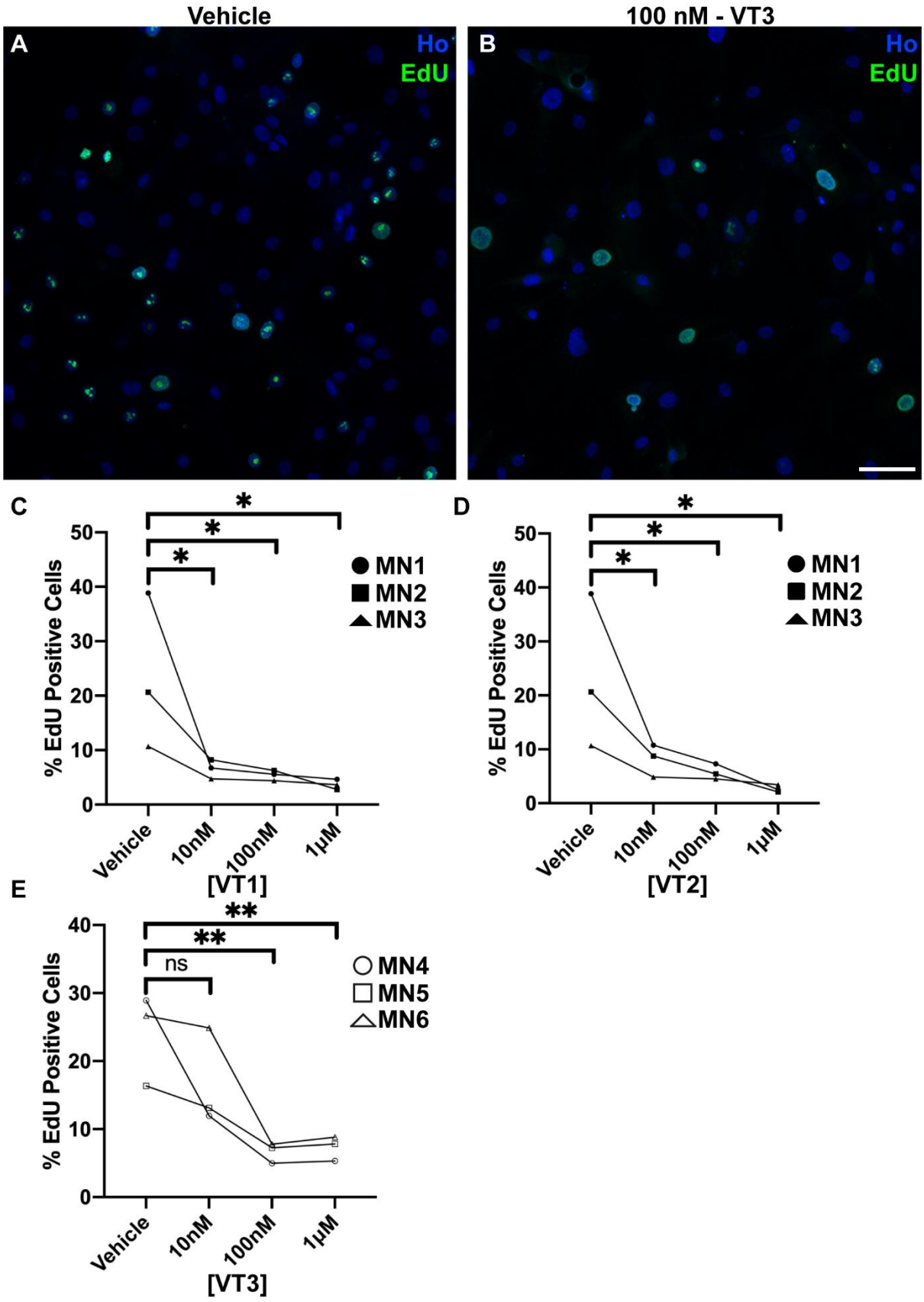

Supplementary Figure 6: TEAD auto-palmitoylation inhibitors reduce proliferation of NF2-null human primary meningioma cells. A, B. Representative immunofluorescence of human primary meningioma cells (MN4 tumour cells shown). Cells were treated with either vehicle (A) or 100 nM VT3 (B) for 48h, EdU positive cells (green) depict proliferating cells, Hoechst (Ho) counterstained nuclei. C-E. Quantification of human primary meningioma cell proliferation with increasing concentrations of auto-palmitoylation inhibitors VT1 (C), VT2 (D) and VT3 (E). Cells from six different human meningioma tumours (MN1-6) were used for this analysis. The proliferation data for each tumour in either vehicle or VT1, VT2 or VT3 inhibitors are shown. N=3 for all data shown. Data are presented as individual data points, and analysis in C-E was one-way ANOVA with Tukey's multiple comparisons test, ns = non-significant, *P<0.05, ** P<0.01. Scale bar: 20 μm

Suppl. Figure 7

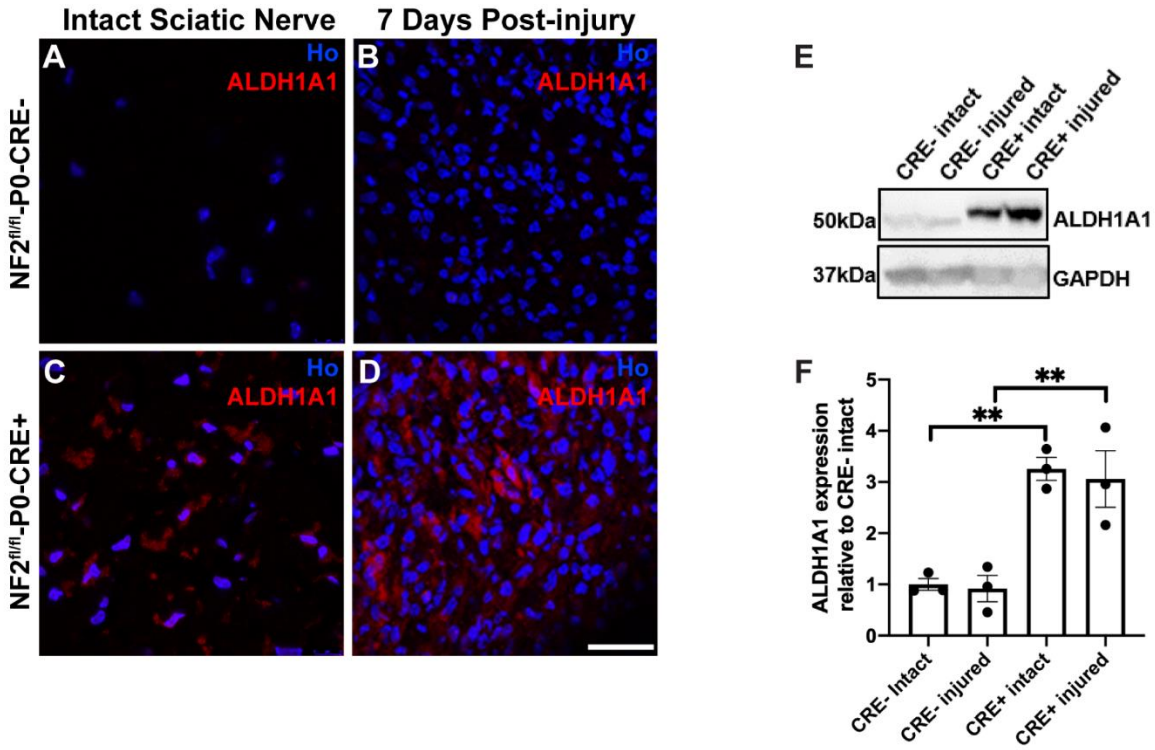

Supplementary Figure 7: ALDH1A1 levels are raised in $NF2^{fl/fl}$/P0-CRE+ mouse sciatic nerve before and after sciatic nerve injury. ALDH1A1 stain of control (A, B; $NF2^{fl/fl}$/P0-CRE-) and NF2 null (C, D; $NF2^{fl/fl}$/P0-CRE+) intact sciatic nerve (A, C) and distal nerve tissue (B, D) at 7 days post-crush injury. E. Western blot of ALDH1A1 protein levels of control (CRE-) and NF2 null (CRE+) intact and 7 days post-crush injury nerves. F. Quantification of western blot in E. For all data, n=3 mice for each genotype and condition. Data presented in graphs are means ±SEM using one way ANOVA with Bonferroni's multiple comparison tests. ** $P<0.01$. Scale bar: 25 μm.

Suppl. Figure 8

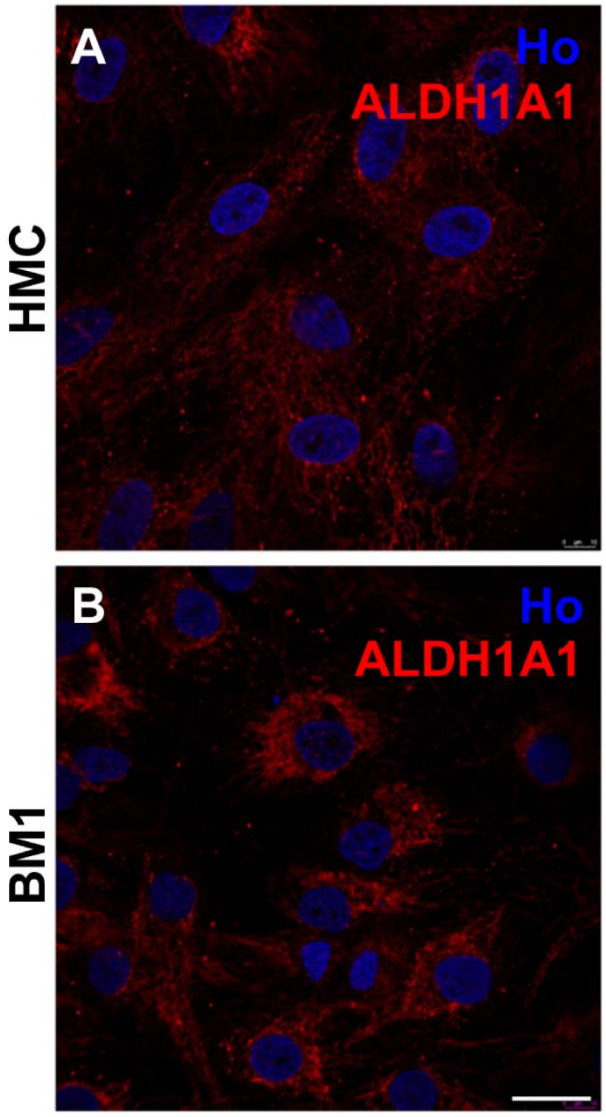

Supplementary Figure 8: Raised levels of ALDH1A1 in NF2-null BenMen-1 meningioma tumour cells (BM1) compared to control human meningeal cells (HMC). A, B. Immunostaining of HMC (A) and BenMen-1 (B) cells with ALDH1A1 antibody. Hoechst counterstain was used to reveal nuclei. Note increased cytoplasmic stain of ALDH1A1 in BenMen-1 cells. n=3 for experiment. Scale bar: 10 μm.

Suppl. Figure 9

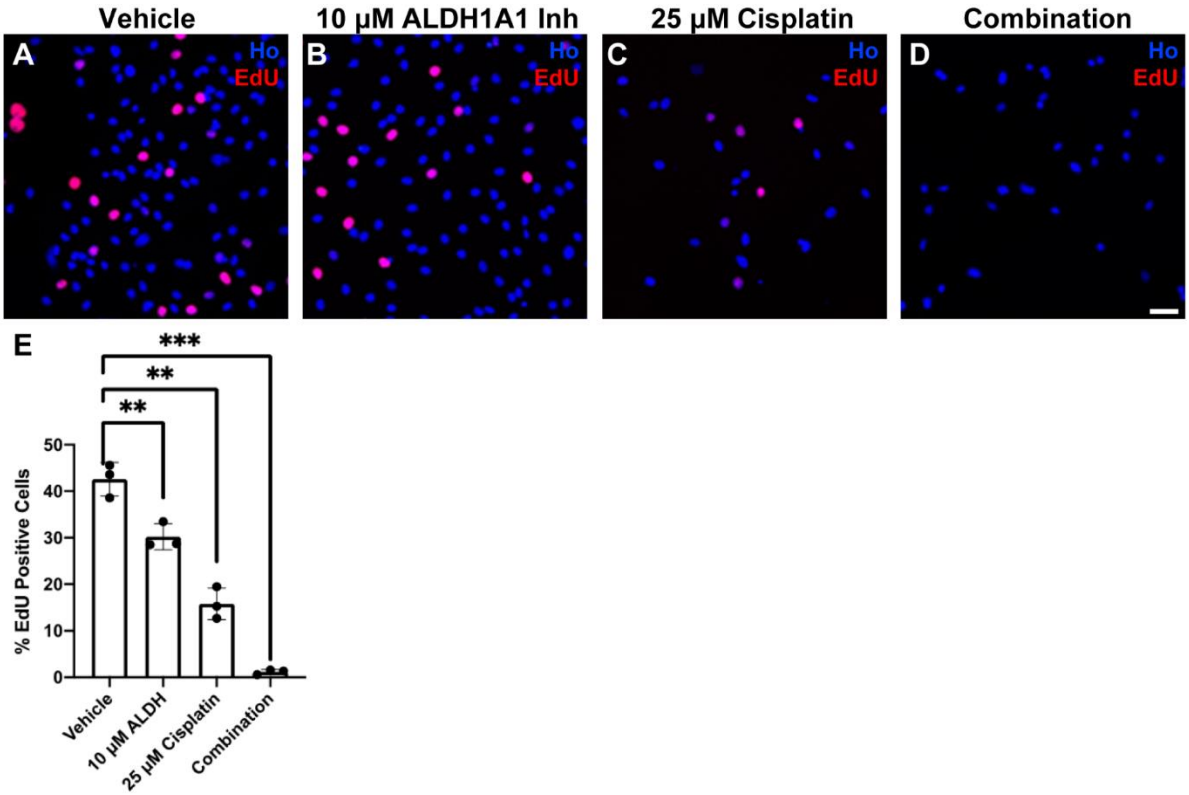

Supplementary Figure 9: The combination of ALDH1A1 inhibitor and cisplatin is highly effective at blocking proliferation of NF2-null BenMen-1 human meningioma cells. A-D. EdU stain of BenMen-1 cells with vehicle (A), 10μM ALDH1A1 inhibitor (B), 25μM cisplatin (C) or 10μM ALDH1A1 inhibitor plus 25μM cisplatin (D). Hoechst counterstain was used to reveal nuclei. E. Quantification of % EdU positive cells with each 48h treatment. Note significant inhibition of proliferation in single treatments, but almost no proliferation with the combination of both treatments. N=3 for all data. Data presented in graphs are means ±SEM using one way ANOVA with Bonferroni's multiple comparison tests. ** $P<0.01$; *** $P<0.001$. Scale bar: 25 μm.

Suppl. Figure 10.

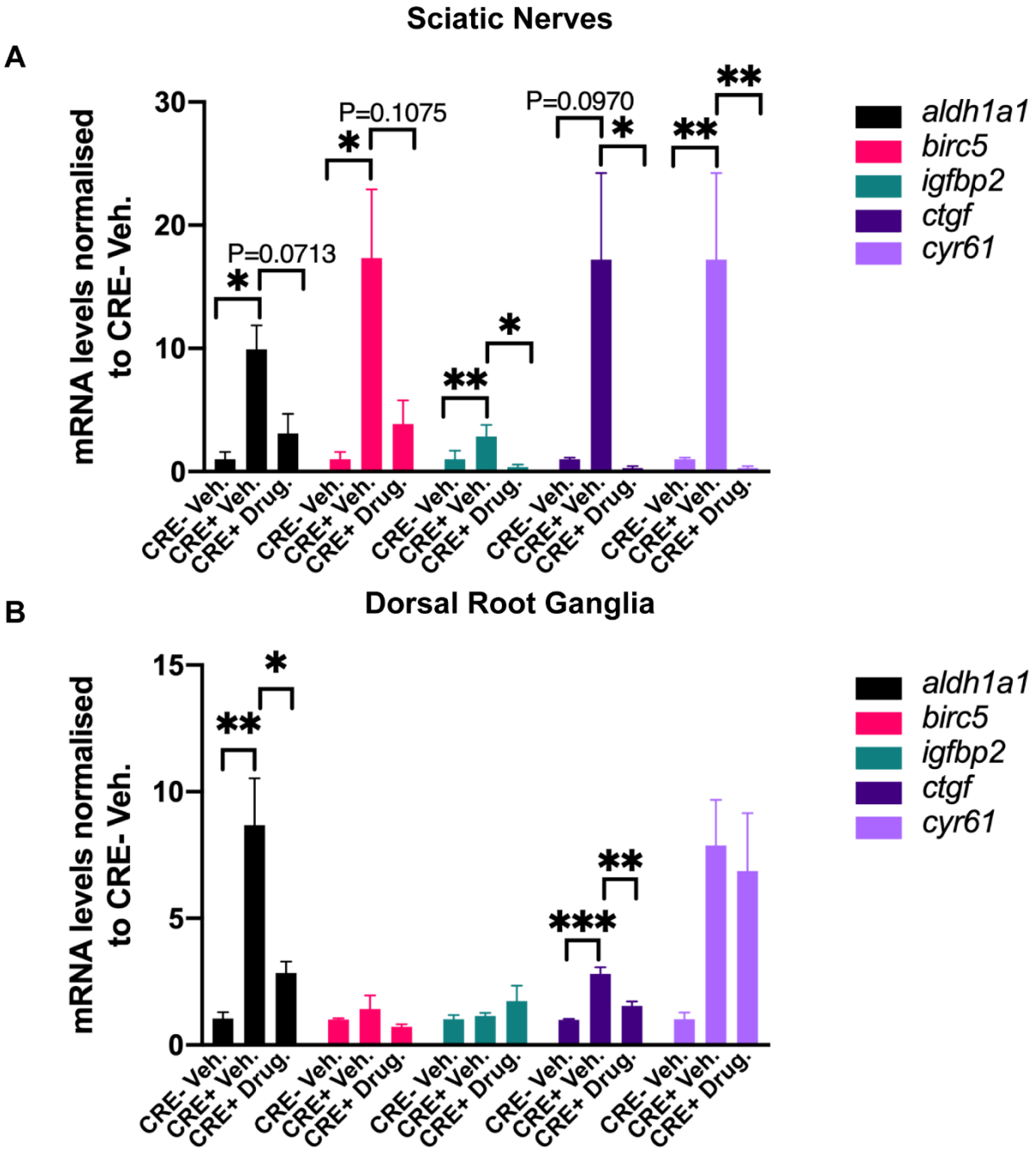

Supplementary Figure 10: Quantitative reverse transcription PCR (qRT-PCR) analysis of Hippo signalling gene targets in sciatic nerves (A) and dorsal root ganglia (DRGs) (B) tissues from CRE- and CRE+ mice. CRE+ animals were treated for 7 days with either vehicle (Veh.) or 30mg/kg of VT2 (Drug) by oral gavage and compared to CRE- vehicle-treated littermate controls. Levels of the Hippo gene targets *aldh1a1, birc5, igfbp2, ctgf* and *cyr61* were determined in samples and shown relative to CRE- vehicle. Data presented in graphs are means ±SEM using one-way ANOVA with Tukey's multiple comparison test.* $P<0.05$; ** $P<0.01$; *** $P<0.001$.

Suppl. Figure 11.

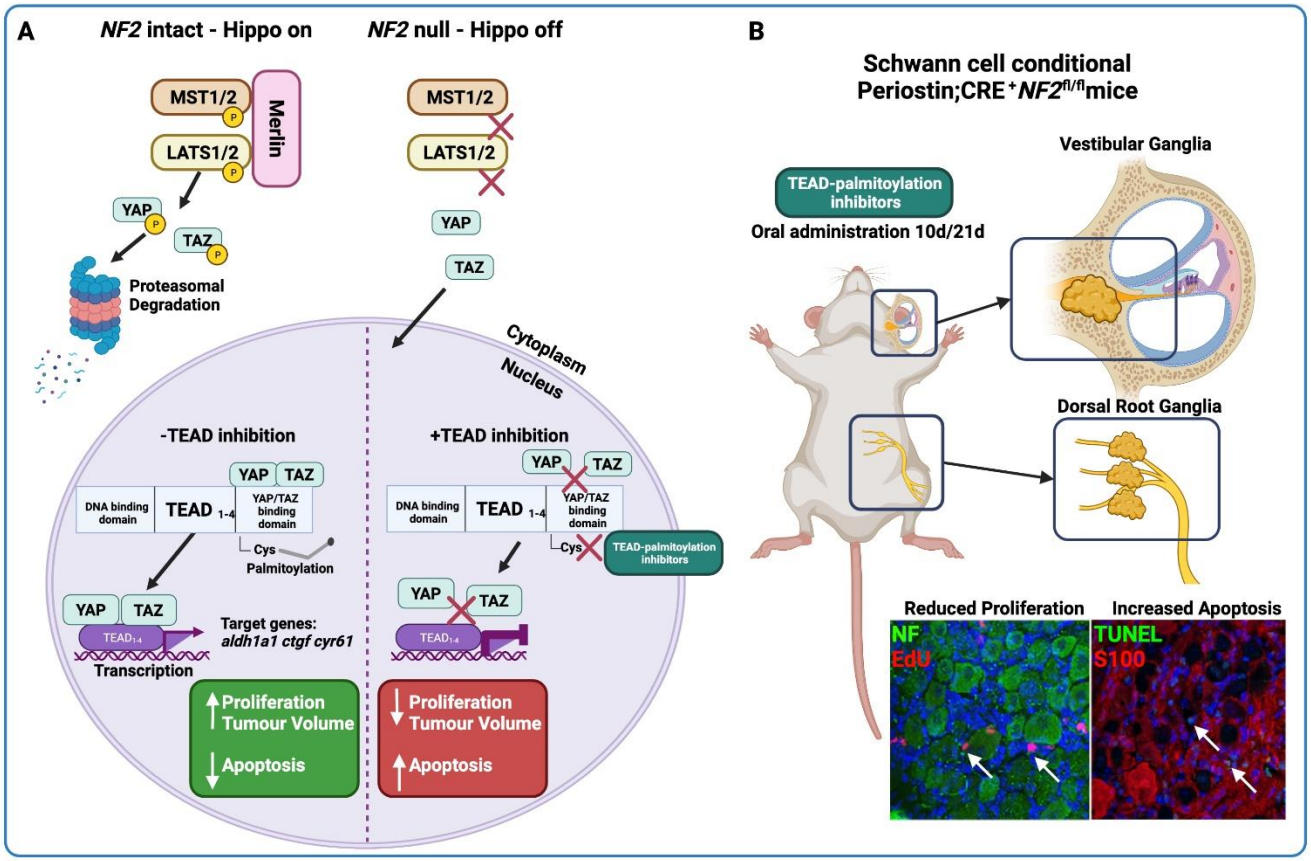

Supplementary Figure 11: TEAD inhibition reduces proliferation and induces apoptosis in the Periostin;$CRE^{+}NF2^{fl/fl}$ schwannoma mouse model. (**A**) Schematic showing the proposed mechanism of small molecule TEAD palmitoylation inhibitors in *NF2*-null schwannoma: In the absence of the *NF2* gene product Merlin, the core kinase cascade of the Hippo pathway remains inactive. Macrophage stimulating protein 1/2 (MST1/2) does not phosphorylate Large tumour suppressor kinase 1/2 (LATS1/2), thus Yes-associated protein (YAP) and WW domain-containing transcriptional regulator protein 1 (TAZ) remain unphosphorylated and are not targeted for proteasomal degradation, but instead translocate into the nucleus. Nuclear YAP and TAZ activate the TEAD family of transcription factors, whereby YAP/TAZ binding is dependent on the palmitoylation of a conserved cysteine residue within the YAP/TAZ binding domain. Small molecule inhibition of this palmitoylation results in downregulation of target genes which drive tumour phenotypes, resulting in a reduction in proliferation and an increase in apoptosis in tumour cells. (**B**) Periostin;$CRE^{+}NF2^{fl/fl}$ mice spontaneously develop schwannomas within their vestibular and dorsal root ganglia. Oral administration of small-molecule TEAD palmitoylation inhibitors results in an increase in apoptosis and decrease in proliferation of schwannoma cells of CRE+ mice.

References.

1. Negroni C, Hilton DA, Ercolano E, et al. GATA-4, a potential novel therapeutic target for high-grade meningioma, regulates miR-497, a potential novel circulating biomarker for high-grade meningioma. *EBioMedicine.* 2020;59:102941.
2. Wang Y, Shan Q, Meng Y, Pan J, Yi S. Mrpl10 and Tbp Are Suitable Reference Genes for Peripheral Nerve Crush Injury. *Int J Mol Sci.* 2017;18(2).
3. Madisen L, Zwingman TA, Sunkin SM, et al. A robust and high-throughput Cre reporting and characterization system for the whole mouse brain. *Nat Neurosci.* 2010;13(1):133-140.